Simultaneous quantitation and confirmation of per- and polyfluoroalkyl substances (PFAS) in food contact materials

Holly Lee[1] and Craig M. Butt[2]
[1] SCIEX, Canada; [2] SCIEX, USA

Introduction

This technical note demonstrates the simultaneous quantitation and identification of PFAS in food contact materials (FCMs) using MRM^{HR} acquisition on the X500R QTOF system. The greater selectivity from high-resolution fragments provided cleaner chromatograms with lower background noise for more sensitive quantitation. At the same time, the high QTOF mass accuracy increased analyte specificity for more confident identification.

Due to their ability to confer oil- and water-repellency, PFAS have been widely reported in FCMs.[2-5] Migration of these chemicals from FCMs into food and food simulants has been extensively demonstrated as a source of dietary exposure.[2,6] While no migration limits have been established for PFAS, Denmark and several US states have passed regulations to ban their use in FCMs.[7,8] Bans such as these necessitate the development of methods that can accurately measure the PFAS concentrations typically present in these materials and be used to confidently confirm these detections to screen for non-compliant products.

Here, targeted MRM^{HR} acquisition was used to quantify and identify PFAS in FCMs with a single injection. In addition to the improved selectivity from monitoring high-resolution fragments, spectral analysis of the MS/MS data provided complementary identification, which helps to mitigate the need for secondary confirmation of PFAS such as perfluorobutanoic acid (PFBA). In this work, an LC-MS/MS method capable of sub-ng/g method detection limits (MDLs) revealed ~90% detection of at least 1 PFAS in all samples tested, including a legacy compound that was phased out of commercial products in the early 2000s (Figure 1).[1]

Key benefits of the analysis of PFAS in FCMs using the X500R QTOF system

- Quantitation based on high-resolution MRM^{HR} fragments produced an LC-MS/MS method with sub-ng/g MDLs achieved for the analysis of 37 PFAS compounds in FCMs
- Confident identification was supported by retention time (RT) confirmation, mass accuracy, spectral library matching and diagnostic fragments
- Positive detection was achieved in ~90% of the FCM samples with total PFAS concentrations up to 55 ng/g, including a legacy PFAS that had been commercially phased out in 2002

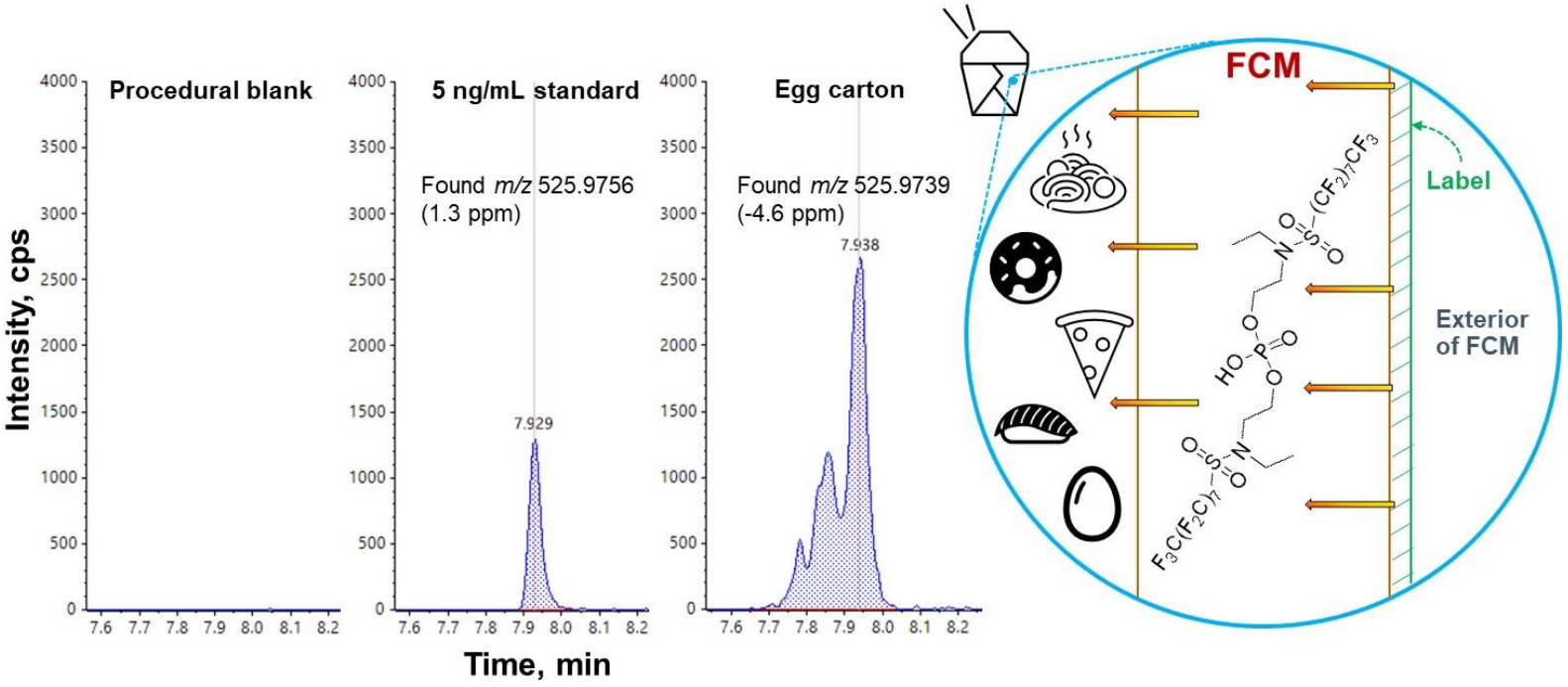

Figure 1. MRM^{HR} extracted ion chromatograms (XICs) of diSAmPAP. MRM^{HR} XICs and fragment mass errors for the diSAmPAP transition (*m/z* 1202.9705 > 525.9763) are presented for the procedural blank, a 5 ng/mL solvent standard and an egg carton extract. Identification was confirmed by RT comparison against authentic standards, ion ratios within 20% and precursor and fragment mass error of <5 ppm.

Experimental methods

Chemicals and samples: The target analyte list consisted of 37 PFAS compounds and mass-labelled internal standards, all purchased from Wellington Laboratories. Individual neat standards were mixed to prepare stock solutions in methanol from which calibration standards (0.1–50 µg/L) were prepared in 80:20 (v/v), methanol/MilliQ water with 10mM ammonium acetate for quantitation. The 34 FCM samples were collected from local retailers and restaurants in 2023 in Toronto, Ontario, Canada. Samples included containers (take-out, fast food, chocolate, candy), pastry bags and liners, produce bags, beverage cups, parchment paper, a popcorn bag, pizza liners and an egg carton.

Sample preparation: The FCM samples were cut into small pieces with masses ranging from 0.2 to 1.5 g. Each sample was spiked with 10 µL of a 500–2000 ng/mL mixed internal standard solution in a polypropylene tube. After adding 15 mL of methanol, the sample was shaken vigorously for 1 hour at 40°C, sonicated for 1 hour and centrifuged for 10 minutes. The supernatant was transferred to a clean polypropylene tube, evaporated to near dryness under nitrogen gas and reconstituted in 0.5 mL of 80:20 (v/v), methanol/MilliQ water with 10mM ammonium acetate for LC-MS/MS analysis. Methanol was extracted in the same manner as laboratory blanks. Kimwipes and an FCM sample (S1, cardboard take-out box) containing low levels of incurred PFAS were used as procedural blanks and quality control (QC) spikes to determine extraction recoveries and MDLs in the matrix.

Chromatography: LC separation was performed on a SCIEX ExionLC AC system using a Phenomenex Luna Omega PS C18 as the analytical column (100 x 2.1 mm, 3 µm, P/N: 00D-4758-AN) and a Phenomenex Luna C18(2) as the delay column (50 x 4.6 mm, 5 µm, P/N: 00B-4252-EO). A flow rate of 0.6 mL/min, an injection volume of 10 µL and a column temperature of 30°C were used. The LC conditions used are shown in Table 1.

Table 1. Chromatographic gradient.

Time (min)	%A	%B
0.0	*80*	*20*
0.5	*80*	*20*
1.0	*45*	*55*
7.0	*1*	*99*
8.0	*1*	*99*
8.1	*80*	*20*
10.0	*80*	*20*

Mobile phase A: MilliQ water with 10mM ammonium acetate
Mobile phase B: Methanol with 10mM ammonium acetate

Mass spectrometry: Analysis was performed using the X500R QTOF system in negative electrospray ionization mode based on the source and gas conditions listed in Table 2.

Table 2. Source, gas and temperature conditions.

Parameter	Value
Polarity	*Negative*
Ion spray voltage	*-4500 V*
Ion source gas 1 (GS1)	*60 psi*
Ion source gas 2 (GS2)	*60 psi*
Curtain gas (CUR)	*40 psi*
Collision gas (CAD)	*10*
Source temperature (TEM)	*550°C*

Data were collected using MRM^{HR} acquisition with the declustering potentials (DP) and collision energies (CE) listed for each analyte in Table 3. The TOF MS scan used a mass range of 100–1225 Da, accumulation time of 0.05 s, DP of -50V and CE of -5V. Due to the large panel of PFAS monitored here, cycle time optimization was necessary to ensure sufficient data point collection across each chromatographic peak for good quantitative performance. As such, the MRM^{HR} transitions were acquired using a single CE by scanning a mass range that covers the fragment ions of each PFAS. Although the selected CE served as a compromise between values that had been optimized for each fragment, this approach enabled the collection of MS/MS spectra for library searching as an additional form of confirmation. For 6:2 diPAP, 8:2 diPAP and diSAmPAP, a narrower mass range was applied to acquire each of their fragments with a specific CE to optimize sensitivity. Retention time scheduling with a tolerance window of 30 seconds was applied to each compound to reduce MRM concurrency for further cycle time optimization.

Data processing: Data were acquired and processed using SCIEX OS software, version 3.1.6. Quantitation was performed based on the MRM^{HR} XICs using the first fragment listed for each analyte in Table 3 as the quantifier transition. For analytes with more than 1 MRM^{HR} transition, the TOF MS precursor and the qualifier transitions were used for confirmation. The SCIEX Fluorochemical HR-MS/MS Spectral Library, version 2.0 was used for library searching against the MS/MS spectra generated from the MRM^{HR} data.

Table 3. Target analyte information for MRM^{HR} acquisition of 37 PFAS compounds listed with their acronyms, molecular formula, exact precursor and fragment masses, DP and CE. Quantitation was performed based on the MRM^{HR} XICs using the first fragment listed as the quantifier transition for analytes with more than 1 MRM^{HR} transition.

Compound	Acronym	Formula	Precursor *m/z*	Fragments *m/z*	DP (V)	CE (V)
Perfluoroalkyl carboxylic acids (PFCAs)						
Perfluorobutanoic acid	*PFBA*	$C_4HF_7O_2$	*212.9792*	*168.9894*	*-25*	*-12*
Perfluoropentanoic acid	*PFPeA*	$C_5HF_9O_2$	*262.9760*	*218.9862*	*-20*	*-12*
Perfluorohexanoic acid	*PFHxA*	$C_6HF_{11}O_2$	*312.9728*	*268.9830, 118.9926*	*-25*	*-20*
Perfluoroheptanoic acid	*PFHpA*	$C_7HF_{13}O_2$	*362.9696*	*318.9798, 168.9894*	*-25*	*-16*
Perfluorooctanoic acid	*PFOA*	$C_8HF_{15}O_2$	*412.9664*	*368.9766, 168.9894*	*-25*	*-18*
Perfluorononanoic acid	*PFNA*	$C_9HF_{17}O_2$	*462.9632*	*418.9734, 168.9894*	*-25*	*-19*
Perfluorodecanoic acid	*PFDA*	$C_{10}HF_{19}O_2$	*512.9600*	*468.9702, 168.9894*	*-25*	*-21*
Perfluoroundecanoic acid	*PFUdA*	$C_{11}HF_{21}O_2$	*562.9568*	*518.9670, 168.9894*	*-25*	*-23*
Perfluorododecanoic acid	*PFDoA*	$C_{12}HF_{23}O_2$	*612.9537*	*568.9638, 168.9894*	*-25*	*-24*
Perfluorotridecanoic acid	*PFTrDA*	$C_{13}HF_{25}O_2$	*662.9505*	*618.9606, 168.9894*	*-25*	*-22*
Perfluorotetradecanoic acid	*PFTeDA*	$C_{14}HF_{27}O_2$	*712.9473*	*668.9574, 168.9894*	*-25*	*-28*
Perfluoroalkane sulfonic acids (PFSAs)						
Perfluorobutane sulfonic acid	*PFBS*	$C_4HF_9O_3S$	*298.9430*	*79.9574, 98.9558*	*-55*	*-49*
Perfluoropentane sulfonic acid	*PFPeS*	$C_5HF_{11}O_3S$	*348.9398*	*79.9574, 98.9558*	*-60*	*-50*
Perfluorohexane sulfonic acid	*PFHxS*	$C_6HF_{13}O_3S$	*398.9366*	*79.9574, 98.9558*	*-60*	*-62*
Perfluoroheptane sulfonic acid	*PFHpS*	$C_7HF_{15}O_3S$	*448.9334*	*79.9574, 98.9558*	*-65*	*-69*
Perfluorooctane sulfonic acid	*PFOS*	$C_8HF_{17}O_3S$	*498.9302*	*79.9574, 98.9558*	*-65*	*-83*
Perfluorononane sulfonic acid	*PFNS*	$C_9HF_{19}O_3S$	*548.9270*	*79.9574, 98.9558*	*-65*	*-92*
Perfluorodecane sulfonic acid	*PFDS*	$C_{10}HF_{21}O_3S$	*598.9238*	*79.9574, 98.9558*	*-65*	*-101*
Perfluoroundecane sulfonic acid	*PFUdS*	$C_{11}HF_{23}O_3S$	*648.9206*	*79.9574, 98.9558*	*-65*	*-132*
Perfluorododecane sulfonic acid	*PFDoS*	$C_{12}HF_{25}O_3S$	*698.9174*	*79.9574, 98.9558*	*-65*	*-141*
Perfluorotridecane sulfonic acid	*PFTrDS*	$C_{13}HF_{27}O_3S$	*748.9143*	*79.9574, 98.9558*	*-65*	*-147*
Perfluoroalkane sulfonamides (FASAs)						
Perfluorobutane sulfonamide	*FBSA*	$C_4H_2F_9NO_2S$	*297.9590*	*77.9655*	*-55*	*-80*
Perfluorohexane sulfonamide	*FHxSA*	$C_6H_2F_{13}NO_2S$	*397.9526*	*77.9655*	*-60*	*-96*
Perfluorooctane sulfonamide	*FOSA*	$C_8H_2F_{17}NO_2S$	*497.9462*	*77.9655*	*-65*	*-115*
Perfluorooctanesulfonamidoacetic acids (FOSAAs)						
N-methyl perfluorooctanesulfonamidoacetic acid	*N-MeFOSAA*	$C_{11}H_6F_{17}NO_4S$	*569.9673*	*418.9734, 482.9353*	*-75*	*-25*
N-ethyl perfluorooctanesulfonamidoacetic acid	*N-EtFOSAA*	$C_{12}H_8F_{17}NO_4S$	*583.9830*	*418.9734, 482.9353*	*-50*	*-33*
Fluorotelomer sulfonates (FTSAs)						
4:2 Fluorotelomer sulfonate	*4:2 FTSA*	$C_6H_5F_9O_3S$	*326.9743*	*306.9681, 80.9652*	*-90*	*-28*
6:2 Fluorotelomer sulfonate	*6:2 FTSA*	$C_8H_5F_{13}O_3S$	*426.9679*	*406.9617, 80.9652*	*-110*	*-35*
8:2 Fluorotelomer sulfonate	*8:2 FTSA*	$C_{10}H_5F_{17}O_3S$	*526.9615*	*506.9553, 80.9652*	*-130*	*-41*
Fluorinated phosphate esters (SAmPAPs and diPAPs)						
6:2 Polyfluoroalkyl phosphate diester	*6:2 diPAP*	$C_{16}H_9F_{26}O_4P$	*788.9751*	*442.9723, 96.9696*	*-65*	*-27, -65*
6:2/8:2 Polyfluoroalkyl phosphate diester	*6:2/8:2 diPAP*	$C_{18}H_9F_{30}O_4P$	*888.9687*	*96.9696*	*-70*	*-70*
8:2 Polyfluoroalkyl phosphate diester	*8:2 diPAP*	$C_{20}H_9F_{34}O_4P$	*988.9623*	*542.9659, 96.9696*	*-75*	*-33, -75*
Perfluorooctanesulfonamidoethanol phosphate diesters	*diSAmPAP*	$C_{24}H_{19}F_{34}N_2O_8PS_2$	*1202.9705*	*525.9763, 649.9682*	*-130*	*-50, -35*
PFAS alternatives						
Hexafluoropropylene oxide dimer acid	*HFPO-DA*	$C_6HF_{11}O_3$	*328.9677*	*284.9779*	*-48*	*-6*
4,8-Dioxa-3H-perfluorononanoic acid	*DONA*	$C_7H_2F_{12}O_4$	*376.9689*	*250.9741, 84.9899*	*-55*	*-25*
9-Chlorohexadecafluoro-3-oxanonane-1-sulfonic acid	*9Cl-PF3ONS*	$C_8HF_{16}ClO_4S$	*530.8956*	*350.9452*	*-120*	*-30*
11-Chloroeicosafluoro-3-oxaundecane-1-sulfonic acid	*11Cl-PF3OUdS*	$C_1HF_{20}ClO_4S$	*630.8892*	*450.9388*	*-160*	*-40*

Quantitative performance of solvent calibration standards

Acceptable calibration performance for accuracy (±30%) and precision (±20%, *n* = 3) was achieved for the calibration standards. Representative results are shown for PFHpA in Figure 2. Overall, the accuracies of the lowest calibration standard at the lower limit of quantitation (LLOQ) were within 30% of the expected value and the %CV values were <20% for triplicate injections. Linear regressions of r^2 ≥0.995 were achieved for the majority of the analytes (Table 4).

Determination of MDLs and recoveries in matrix spikes

MDLs were calculated by performing 8 replicate low-level spikes in a blank FCM (S1) sample previously determined to have little or no incurred PFAS present. The MDL was calculated by multiplying the standard deviation from the 8 replicates by the t-value (2.998) at the 99% confidence level, as follows:

$$MDL = s \; x \; t_{(n\text{-}1,\, 1\text{-}\alpha=0.99)}$$

A series of text-based and calculated columns was used to derive the custom formula based on the above equation to calculate the in-vial MDL, which was then converted to the mass-based MDL based on the reconstitution volume and extracted sample mass (Figure 2). Table 4 lists the mass-based MDLs for the target PFAS, most of which were <0.5 ng/g. The observed mass-based MDLs provided sufficient sensitivity for the quantitative analysis of FCMs for which concentrations typically range from tens to thousands of ng/g.[2-4]

The majority of the analytes demonstrated acceptable apparent recoveries in the range of 70%–130% with %CV <20% measured at 2 spiking levels in the blank FCM (S1) and Kimwipe matrices (Table 4). Isotope-labeled internal standards spiked prior to the extraction were used to correct these recoveries for losses and matrix effects, although some analytes used surrogate internal standards due to the lack of a mass-labelled analogue. Recoveries would likely improve further with the use of additional matching mass-labelled internal standards.

Due to the background presence of PFHpA in Kimwipes, MDL determination could not be performed at the required low levels in this matrix. Instead, absolute recoveries were determined by calculating the quotient of the peak areas in Kimwipes spiked before and after extraction to assess recovery loss. Overall, acceptable absolute recoveries of 80%–120% with %CV <20% were achieved for the majority of the analytes (Table 4).

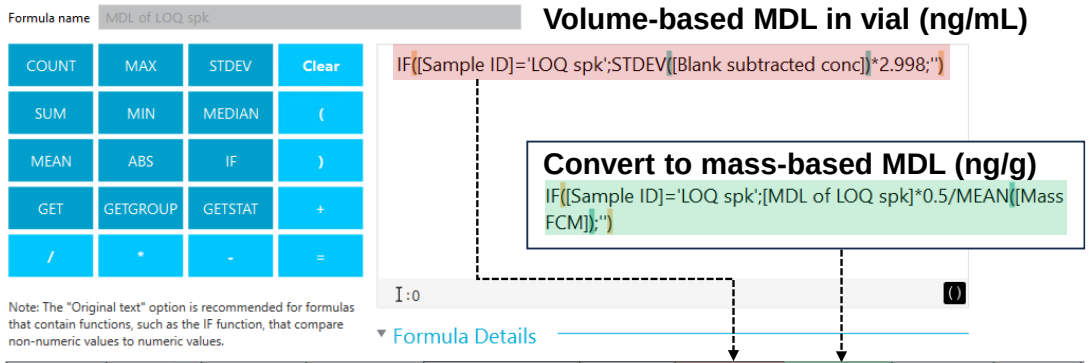

Index	Sam... Name	Sample ID	Compo... Name	*Blank subtracted conc	*Mass FCM	*MDL of LOQ spk	*MDL mass-...	*Mean of Ap...	*%CV of...
1617	LB		PFHpA_1						
1751	MB		PFHpA_1						
1885	MS1	LOQ spk	PFHpA_1	1.887	0.7347	0.42	0.28	92.3	7.7
2019	MS2	LOQ spk	PFHpA_1	1.915	0.7785	0.42	0.28	92.3	7.7
2153	MS3	LOQ spk	PFHpA_1	1.673	0.7546	0.42	0.28	92.3	7.7
2287	MS4	LOQ spk	PFHpA_1	1.833	0.7455	0.42	0.28	92.3	7.7
2421	MS5	LOQ spk	PFHpA_1	1.686	0.7742	0.42	0.28	92.3	7.7
2555	MS6	LOQ spk	PFHpA_1	2.086	0.7156	0.42	0.28	92.3	7.7
2689	MS7	LOQ spk	PFHpA_1	1.943	0.7460	0.42	0.28	92.3	7.7
2823	MS8	LOQ spk	PFHpA_1	1.744	0.7646	0.42	0.28	92.3	7.7

Figure 2. Screenshots demonstrating custom calculations in SCIEX OS software. Custom formulas (top) were used to calculate the volume- (red) and mass-based (green) MDLs of PFHpA from replicate spikes based on text-based and calculated columns in the results table (bottom).

Table 4. Quantitative method performance for solvent calibration standards and matrix spikes. The dynamic range, regression coefficient (r^2), MDLs, apparent recoveries at 2 spiking levels in the S1 (cardboard take-out) and Kimwipe samples and absolute recoveries at 1 spiking level in the Kimwipe sample are listed.

Compound	Internal standard	Calibration range (ng/mL)	Linearity (r^2)	MDL (ng/g)	Apparent recovery (%Rec (%CV)) Internal standards-normalized			Absolute recovery (%Rec (%CV))
					1 ng in S1 (n = 8)	1 ng in Kimwipe (n = 8)	10 ng in Kimwipe (n = 3)	10 ng in Kimwipe (n = 3)
PFBA	$^{13}C_4$-PFBA	0.1 – 50	0.998	0.22	94.4 (5.9)	98.7 (2.6)	101 (5.4)	114 (16.3)
PFPeA	$^{13}C_5$-PFPeA	0.1 – 50	0.995	0.22	101 (5.4)	99.7 (3.1)	102 (4.8)	119 (14.7)
PFHxA	$^{13}C_5$-PFHxA	0.5 – 50	0.997	0.24	96.5 (6.1)	99.6 (5.3)	99.0 (3.2)	115 (7.6)
PFHpA	$^{13}C_4$-PFHpA	0.1 – 50	0.996	0.28	92.4 (7.6)	-	105 (3.0)	99.0 (17.9)
PFOA	$^{13}C_8$-PFOA	0.1 – 50	0.997	0.24	90.1 (6.5)	104 (4.8)	100 (2.5)	111 (11.9)
PFNA	$^{13}C_9$-PFNA	0.1 – 50	0.998	0.23	98.6 (5.9)	103 (6.1)	99.4 (5.6)	112 (16.4)
PFDA	$^{13}C_6$-PFDA	0.1 – 50	0.995	0.23	102 (5.7)	102 (3.5)	96.8 (1.5)	116 (15.1)
PFUdA	$^{13}C_7$-PFUdA	0.1 – 50	0.996	0.35	96.7 (9.0)	104 (3.7)	106 (11.5)	104 (7.8)
PFDoA	$^{13}C_2$-PFDoA	0.1 – 50	0.996	0.17	97.9 (4.3)	103 (4.3)	109 (8.4)	110 (14.7)
PFTrDA	$^{13}C_2$-PFDoA	0.1 – 50	0.995	0.14	*67.4 (5.3)	101 (9.6)	97.4 (9.3)	105 (19.9)
PFTeDA	$^{13}C_2$-PFDoA	0.1 – 50	0.996	0.23	88.9 (6.6)	95.8 (9.2)	95.5 (18.7)	109 (15.7)
PFBS	$^{13}C_3$-PFBS	0.1 – 50	0.997	0.24	112 (5.5)	107 (6.1)	107 (2.4)	114 (15.6)
PFPeS	$^{13}C_3$-PFBS	0.1 – 50	0.998	0.72	122 (14.6)	106 (8.8)	91.9 (3.3)	118 (14.7)
PFHxS	$^{13}C_3$-PFHxS	0.1 – 50	0.995	0.27	111 (6.2)	103 (5.1)	108 (2.8)	108 (16.4)
PFHpS	$^{13}C_3$-PFHxS	0.5 – 50	0.997	0.26	119 (5.4)	107 (6.2)	102 (6.6)	114 (10.2)
PFOS	$^{13}C_8$-PFOS	0.5 – 50	0.996	0.26	102 (6.2)	102 (7.6)	89.7 (4.4)	112 (11.2)
PFNS	$^{13}C_6$-PFDA	0.5 – 50	0.995	0.66	*131 (12.6)	90.2 (10.3)	91.0 (6.4)	117 (13.3)
PFDS	$^{13}C_7$-PFUdA	0.5 – 50	*0.993	0.28	116 (6.1)	97.2 (6.4)	102 (9.5)	107 (19.8)
PFUdS	$^{13}C_2$-PFDoA	0.1 – 50	0.999	0.28	102 (6.9)	83.1 (5.0)	74.2 (8.6)	102 (4.2)
PFDoS	$^{13}C_2$-PFDoA	0.5 – 50	*0.994	0.31	72.1 (10.7)	95.2 (7.2)	80.7 (6.0)	95.2 (4.6)
PFTrDS	$^{13}C_2$-PFDoA	0.1 – 50	0.998	0.19	95.4 (5.1)	85.3 (4.1)	75.2 (3.9)	105 (*28.7)
FBSA	$^{13}C_3$-PFBS	0.5 – 50	0.995	0.32	70.3 (11.3)	*53.0 (27.1)	*61.8 (3.0)	85.4 (14.7)
FHxSA	$^{13}C_3$-PFHxS	0.5 – 50	0.995	0.24	*64.7 (9.5)	*61.9 (14.1)	70.5 (3.5)	90.2 (11.3)
FOSA	$^{13}C_8$-PFOS	0.5 – 50	*0.992	0.31	70.9 (10.8)	73.9 (12.8)	72.3 (7.3)	102 (12.7)
N-MeFOSAA	$^{13}C_7$-PFUdA	0.5 – 50	0.995	0.35	121 (7.3)	81.8 (8.0)	107 (3.1)	127 (4.6)
N-EtFOSAA	$^{13}C_7$-PFUdA	0.5 – 50	0.996	0.52	*139 (9.3)	99.9 (6.1)	111 (3.5)	122 (17.3)
4:2 FTSA	$^{13}C_2$-4:2FTSA	0.5 – 50	0.997	0.28	110 (6.4)	108 (5.2)	108 (0.4)	113 (14.4)
6:2 FTSA	$^{13}C_2$-6:2FTSA	0.5 – 50	0.996	0.30	*134 (5.6)	121 (4.1)	106 (4.1)	112 (14.6)
8:2 FTSA	$^{13}C_2$-8:2FTSA	0.5 – 50	0.995	0.42	*135 (7.8)	114 (8.8)	113 (7.7)	118 (18.7)
6:2 diPAP	$^{13}C_2$-PFDoA	0.5 – 50	*0.992	0.62	130 (12.1)	129 (18.1)	85.4 (2.9)	114 (19.1)
6:2/8:2 diPAP	$^{13}C_2$-PFDoA	0.5 – 50	*0.994	0.24	*145 (4.2)	*148 (10.8)	74.9 (7.2)	117 (19.1)
8:2 diPAP	$^{13}C_2$-PFDoA	0.5 – 50	*0.994	0.76	*147 (12.9)	117 (8.4)	84.5 (1.8)	115 (12.1)
diSAmPAP	$^{13}C_2$-PFDoA	0.5 – 50	*0.992	0.45	127 (8.9)	97.1 (8.7)	116 (5.8)	130 (12.2)
HFPO-DA	$^{13}C_3$-HFPO-DA	0.5 – 50	0.997	0.33	110 (7.6)	103 (6.6)	103 (3.9)	117 (12.6)
DONA	$^{13}C_3$-HFPO-DA	0.1 – 50	0.998	0.44	*143 (7.7)	115 (6.3)	99.1 (7.6)	106 (15.3)
9Cl-PF3ONS	$^{13}C_6$-PFDA	0.1 – 50	0.995	0.45	111 (10.2)	95.0 (9.1)	93.0 (6.7)	113 (14.0)
11Cl-PF3OUdS	$^{13}C_2$-PFDoA	0.1 – 50	0.995	0.15	89.5 (4.1)	93.0 (7.1)	112 (5.1)	112 (19.8)

Note: Apparent recovery of PFHpA in the Kimwipe sample could not be determined because the background presence of the analyte interfered at the 1 ng spiking level

Note: Acceptable method performance for linearity (r^2 ≥0.995), recovery (±30%) and precision (±30% in 1 ng spike, ±20% in 10 ng spike) was achieved for the majority of the analytes, except for those denoted with an asterisk

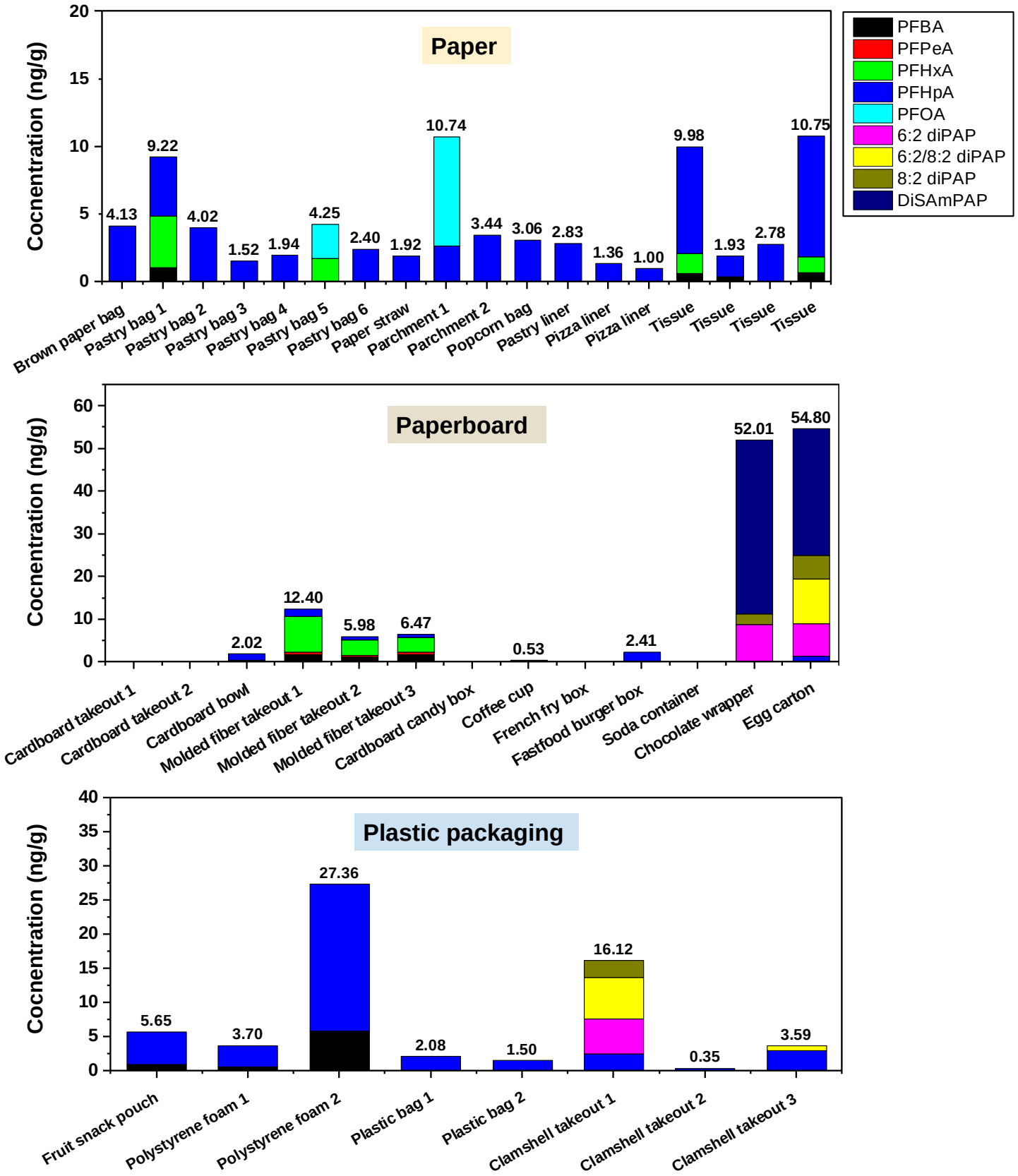

Figure 3. Concentrations of PFAS (ng/g) in 3 different types of FCMs. The total PFAS concentrations are listed at the top of each FCM sample. The total PFAS concentrations were calculated as a sum of the individual congener concentrations.

Simultaneous quantitation and confirmation of PFAS in FCMs

Almost 90% of the FCM samples exhibited positive detection of at least 1 PFAS compound with PFHpA as the dominant congener (82%), followed by PFBA (31%) and PFHxA (18%). PFPeA, PFOA, diPAPs and diSAmPAP were occasionally (<10%) detected. This distribution aligns with the industrial transition from the longer chain compounds to the 6:2 fluorotelomer-based chemistries and the congener profiles previously reported in FCMs.[2-4] Figure 3 shows the PFAS concentrations observed in different food packaging materials. Compound identification in each sample was confirmed by RT comparison against standards, ion ratios within 20%, precursor and fragment mass error within 5 ppm and spectral MS/MS analysis (Figure 4). Short-chain PFAS, such as PFBA, lack secondary MRM transitions which are typically used for confident compound confirmation and novel PFAS identification. In the current workflow, this was achieved through interrogation of the MS/MS spectra against published or literature reference spectra.

Both the diPAPs and diSAmPAP compounds were detected in a recyclable plastic clamshell box, a cardboard chocolate wrapper and an egg carton at concentrations ranging from 2.3 to 41 ng/g. The levels of diPAPs observed here are consistent with their use as greaseproofing agents in FCMs and with concentrations previously reported.[2-5] In contrast, the detection of diSAmPAPs in the chocolate wrapper and egg carton, both of which were comprised of recycled paper fiber, was unexpected. The diSAmPAPs were historically used as FCM components until perfluorooctylsulfonyl (POSF)-based chemistries were phased out in North America in 2002,[1] although production may still persist in Asia.[9]

The diSAmPAP levels observed can only be considered semi-quantitative because both the branched and linear isomers were observed in the samples, whereas the analytical standard used for quantitation only contained the linear isomer. Figure 1 shows the XIC comparison for the procedural blank, a 5 ng/mL solvent calibration standard and an egg carton extract. The merged peaks comprised of the branched (RT of 7.85 min) and linear (RT of 7.95 min) isomers were integrated to semi-quantify diSAmPAP against the linear analytical standard. Identification of diSAmPAP was further authenticated by the presence of 2 diagnostic fragments (*m/z* 525.9763 and 649.9682) that had been previously reported in published MS/MS spectra.[5]

Overall, the total PFAS concentrations ranged from <MDL to 55 ng/g. The higher PFAS levels were typically observed in FCMs made of molded plant fiber, which suggests that recycled paper is a potential contamination source. Other potential sources of contamination include the intentional use of PFAS as greaseproofing agents to confer oil- and water-repellency or as dispersion aids in the printing inks used on FCMs.

Conclusions

- Using the X500R QTOF system, MRM^{HR} acquisition was used to simultaneously quantify and confidently identify PFAS in food packaging materials in the same injection
- Compound identification was supported by mass accuracy, isotope ratio pattern, diagnostic fragments, spectral MS/MS matches and RT matches against authentic standards
- Quantitation based on MRM^{HR} XICs enabled sub-ng/g MDLs and revealed total PFAS concentrations ranging from <MDL to 55 ng/g in the FCMs. Two samples contained diSAmPAP, a legacy PFAS that is no longer in production in North America.

References

1. Phase-out Plan for POSF-based Products; U.S. EPA Public Docket AR226-0600, OPPT-2002-0043; 3M Specialty Materials Markets Group: St. Paul, MN, 2000.
2. Sapozhnikova, Y. *et al.* Assessing per- and polyfluoroalkyl substances in globally sourced food packaging. *Chemosphere.* **2023**, *337*, 139381.
3. Schwartz-Narbonne, H. *et al.* Per- and Polyfluoroalkyl Substances in Canadian Fast Food Packaging. *Environ. Sci.: Technol. Lett.* **2023**, *10*, 343-349.
4. Straková, J. *et al.* Throwaway Packaging, Forever Chemicals: European wide survey of PFAS in disposable food packaging and tableware. 54 p.
5. Bugsel, B. *et al.* LC-HRMS screening of per- and polyfluorinated alkyl substances (PFAS) in impregnated paper samples and contaminated soils. *Anal. Bioanal. Chem.* **2021**, *414*, 1217-1225.
6. Begley, T.H. *et al.* Migration of fluorochemical paper additives from food-contact paper into foods and food simulants. *Food Addit. Contam.* **2008**, *25*, 384-390.
7. Boucher, J. Denmark moves ahead with PFAS bans in FCMs. Food Packaging Forum, May 29 2020.
8. Parkinson, L. US state actions concerning food packaging and chemicals in 2023. Food Packaging Forum, July 20 2023.
9. Martin, J.W. *et al.* PFOS or PreFOS? Are perfluorooctane sulfonate precursors (PreFOS) important determinants of human and environmental perfluorooctane sulfonate (PFOS) exposure? *J. Environ. Monit.* **2010**, *12*, 1979-2004.

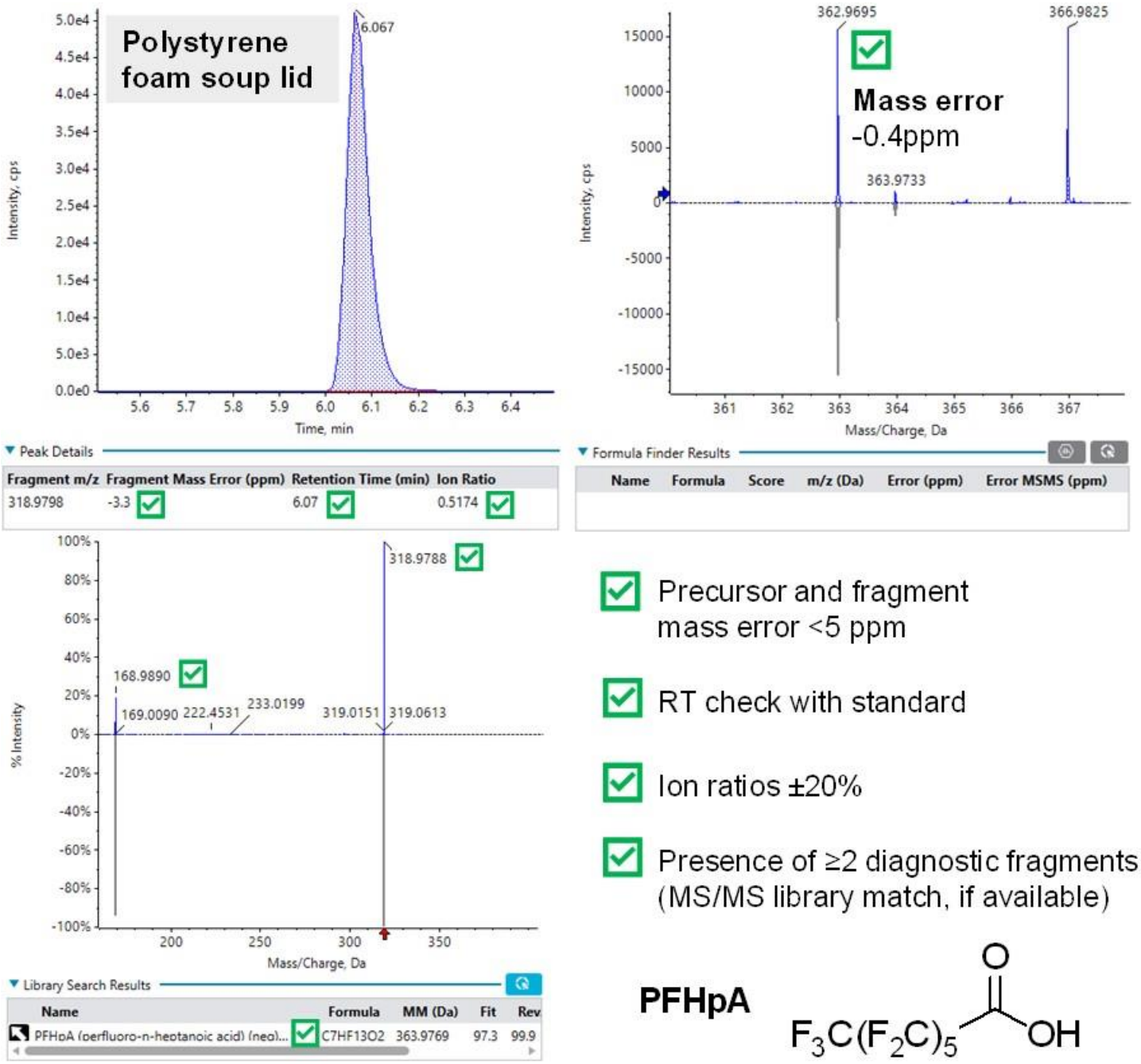

Figure 4. Confirmation of PFHpA in an extract of a polystyrene foam lid. The MRM^{HR} XIC with the fragment mass error, RT and ion ratio for the PFHpA quantifier transition (*m/z* 362.9696 > 318.9798) is shown on the top left. The top right shows the TOF MS spectrum with the precursor mass error. The bottom shows the comparison of the experimental TOF MS/MS spectrum against the library spectrum with the identified library hit and score at the bottom.

Headquarters
500 Old Connecticut Path | Framingham, MA 01701 USA
Phone 508-383-7700
sciex.com

International Sales
For our office locations please call the division headquarters or refer to our website at
sciex.com/offices